Available online at www.sciencedirect.com
SCIENCE DIRECT®
Microelectronic Engineering 83 (2006) 990–993
MICROELECTRONIC ENGINEERING
www.elsevier.com/locate/mee

Advances in microchannel amplifiers for maskless lithography

Anton S. Tremsin *, David R. Beaulieu, Harry F. Lockwood

Arradiance, Inc., 142 North Road, Suite F-150, Sudbury, MA 01776, USA

Available online 3 March 2006

Abstract

Arradiance is developing a novel approach for achieving the high brightness and intra-field beam uniformity required for volume production electron beam maskless lithography. The goal is to utilize an electron multiplying array operating in saturation to amplify, stabilize and control the output of an array of cold cathodes. The authors discuss advancements in both theoretical and experimental methods to characterize and optimize the channel structure of silicon based microchannel amplifiers (MCAs) operating both near and in deep saturation. Combined with experimental data from fabricated prototypes, this paper reports the recent results of new methodologies in modeling on both a macroscopic and a microscopic scale. This will enable the prediction and optimization of key operational parameters. In addition, new experimental methodologies have been developed to quantify the transfer characteristics of individual channels within large arrays. These new methods offer the high level of predictive capability required for both device optimization and fabrication control necessary to achieve lithography level source performance.
© 2006 Elsevier B.V. All rights reserved.

Keywords: Maskless lithography; Microchannel amplifier; Source brightness and uniformity

1. Introduction

Traditional optical lithography requires production of a set of masks, which becomes more and more expensive with recent advancements to sub-100 nm technology. Among alternatives to well-established optical lithography there are a few approaches, such as nanoimprint lithography, optical and charged-particle maskless lithographies [1]. Direct electron beam pattern writing is used in a few novel approaches, some of which are being developed at the present time [2–4]. While the pattern feature sizes written by an electron beam can be as small as 10 nm, its applicability to lithography is limited by the writing speed of a single electron beam. That limitation can be overcome by utilization of massively parallel system with large number of independently controlled (and/or blanked) beams. One of such approaches developed by Arradiance utilizes a large array of cold-cathode emitters amplified, stabilized and controlled by a microchannel electron multiplying array (MCA), followed by an electron beam lens array focusing and deflecting beams, Fig. 1. The electron beams in such a system are individually switchable at the cold cathode emitter (low voltage control signals) and do not require any further beam blanking and should not exhibit any crosstalk. The ~14,000 beams in the developed system will be on 250 μm grid covering 26×33 mm^2 field and will each provide ~1.2 nA current within a 45-nm spot at the wafer. In order to achieve the high brightness and uniformity required for maskless lithography, the MCA performance must be optimized simultaneously across a large field. In the present paper, we concentrate on the optimization of MCA parameters and techniques for experimental characterization.

2. MCA based electron source

Channel electron amplifiers have been widely used in detection systems over the last 30 years. A large number of articles have been published on both theoretical (e.g., [5–7]) and experimental studies (e.g., [8,9]) of glass microchannel plates, widely used in image intensified and night vision devices. However, the fabrication of similar devices with lithographic precision and their operation in deep

* Corresponding author. Tel.: +1 978 369 8292; fax: +1 978 369 8239.
E-mail address: atremsin@arradiance.com (A.S. Tremsin).

0167-9317/$ - see front matter © 2006 Elsevier B.V. All rights reserved.
doi:10.1016/j.mee.2006.01.261

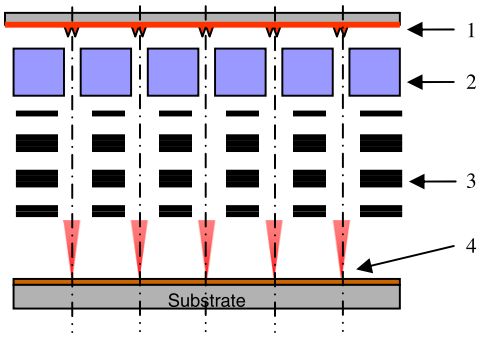

Fig. 1. Schematic diagram of the proposed lithography source. 1 – switchable field emission tip array; 2 – microchannel amplifier array; 3 – integrated microcolumn electrostatic lens array; 4 – focused e-beam array.

saturation as a controlled source of electron beams has not been fully explored. Detection devices typically require operation of channel amplifiers at relatively high gain on an event-by-event basis (e.g., photon counting detection). In contrast, the MCA has to operate in a current amplifying mode and should provide stability and beam uniformity across a large field, while the amplification factor can be relatively small. In most detection applications, the intensity of amplified signal should be proportional to the intensity of incoming signal, while the MCA output should be very stable and uniform across the entire array. The latter distinction allows for the operation of the MCA in, or near, deep saturation, while in most detection devices the saturation of the output signal of channel electron amplifiers has to be avoided [5,6,8].

3. Source optimization through modeling

Despite the fact that the MCA is engineered on a lithographically etched silicon wafer, its operation is quite similar to that of glass microchannel plates (MCPs). Therefore models of the amplification process inside an MCP pore, in particular macroscopic models of amplification, saturation [5,6] and microscopic models of electron avalanche [7,10], can be adopted to modeling of the MCA performance.

3.1. Macroscopic model of MCA saturation

Our MCA saturation model is based on MCP models [5,6] and approximates the amplification process by continuous equations of current conservation; it predicts the value of the output current as a function of input current and accelerating voltage for a given MCA's pore resistance and length. The model has only two input parameters, characterizing all the secondary electron emission parameters of pore surface: the gain, G, per pore unit length and the voltage V_m at which the gain is equal to unity. These two parameters have to be determined by fitting the modeled data to measured MCA gain curves. Our first experimental studies of MCA prototypes indicate that the parameters G and V_m are very close to relatively well-determined values for microchannel plates. The macroscopic

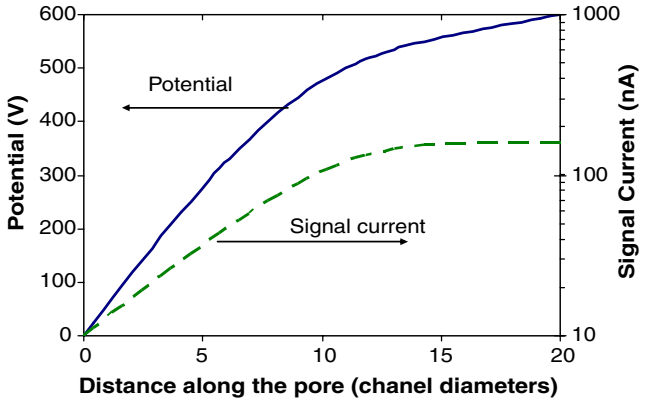

Fig. 2. Calculated potential distribution along the MCA pore and signal current as a function of position along the pore. Saturation leads to non-linear potential distribution. Signal is amplified only in the first half of the pore.

model not only predicts the value of output ("signal") current, but also its value along the pore. In deep saturation, the amplification of the electrons happens only in the initial section of an MCA pore, while the rest of the pore operates at a gain of unity. Thus, signal current increases rapidly along the input section of the MCA pore, and then remains almost constant, Fig. 2. It is that signal saturation that reduces the fluctuations of the signal from cathode emitters and allows the production of a stable source required for lithography. With the help of the saturation model, we can optimize not only the source stability, but also other MCA operational parameters such as the absolute value of input current, MCA gain and, as a result, the thermal load, which, in turn, depends on the level of saturation.

The macroscopic model is also used for determination of MCA fabrication tolerances in order to preserve 2% uniformity across the entire array. Omitting detailed description of the latter process and particular values for each fabrication step, we just summarize here that the modeling proves the fabrication tolerances are all within achievable values for current technologies involved in manufacturing the MCA. We also envision engineering an MCA with variable resistivity along the pore, in order to reach saturation for lower input currents or accelerating voltages (opposite to what was proposed for MCP detection devices where the saturation is to be circumvented [5]). The same effect can also be achieved by stacking of several MCAs fabricated with different fixed resistivities. The potential distributions along the pore in such an MCA (at zero input current) are shown in Fig. 3 for two opposite orientations. Thus, setting the operational and manufacturing parameters in accordance to the predicted values, we should be able to optimize the stability and uniformity of output current.

3.2. Microscopic 3D Monte-Carlo modeling of MCA output distributions

The macroscopic model described in the previous section predicts the value of the output current, but not the

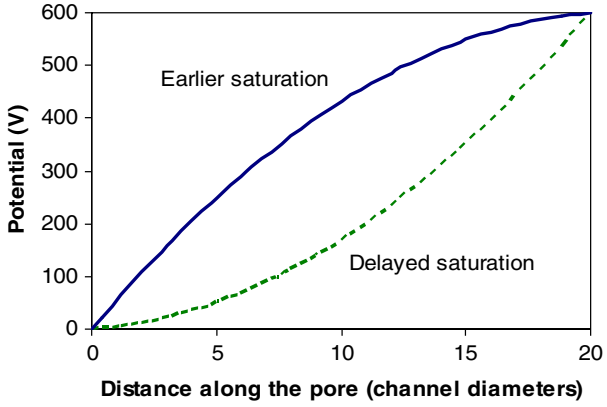

Fig. 3. Calculated potential distribution along the pore with variable resistivity. Resistivity linearly decreases from 3E5 to 2E4 Ω cm (solid line) and linearly increases from 2E4 to 3E5 Ω cm (dashed line) along the pore.

brightness of the source. It also does not take into account the discrete nature of the amplification process, which has to be considered on order to estimate the output distributions. Previous microscopic modeling attempts followed the electron trajectories inside the pore in a two-dimensional geometry [7] instead of a full three-dimensional consideration. Despite this simplification, the model required extensive computational power and therefore the number of modeled wall collisions was very small (<100). Due to the statistical nature of the electron amplification process, the number has to be several orders of magnitude larger in order to predict the MCA brightness with reasonable accuracy. We are currently developing a full three-dimensional Monte-Carlo model that traces the primary and secondary electrons traversing the channel and generating new secondaries upon the collision with the channel wall. For this, we are using secondary electron emission distributions adopted from available data in the literature. Currently our microscopic model predicts the output energy and angle for each electron at the pore exit, taking into account the perturbation of the static accelerating electric field by the end electrodes. Generating sufficient output electrons allows for the prediction of MCA output parameters for a given accelerating voltage (across the pore and between the MCA and focusing electron optics) and pore geometry (length/diameter, endspoiling electrodes). Presently, only the unsaturated pore can be modeled; the model is being updated to take into account the buildup of positive wall charges in order to simulate the pore operation in saturation. Once the model is updated, we will use it to optimize the source brightness by varying the MCA structural (pore geometry, electrode end spoiling, resistance) and operational (accelerating biases, input current, level of saturation) parameters in order to achieve the highest source brightness and uniformity.

4. Experimental metrology

The performance of the proposed source for maskless lithography ultimately has to be characterized experimentally. The requirement on source uniformity to be within 2% across the field necessitates the 2% uniformity of source to be used in calibration. At the same time, the value of the output current can be measured with accuracy not better than the accuracy of the input current entering an individual MCA pore with dimensions on the scale of ~10 μm. The column of a secondary electron microscope (SEM) seems to be close to an ideal source for MCA calibration. Not only is the electron beam well calibrated and stable in time, it can also be focused into a single pore ensuring the measured accuracy of the input current. The beam can be scanned from pore to pore and thus the uniformity of MCA operation can be calibrated across the entire field. Fig. 4 shows the schematic diagram of the experimental setup for the measurements of output current and uniformity. The MCA is tilted to a controlled angle, thus providing the possibility to inject the electron beam into a given area along the pore. Changing the tilt angle, the gain profile along the pore can be measured with some accuracy. The SEM column current is calibrated by a Faraday cup. That system is being currently updated to perform the measurements of the source brightness. Our first measurements of the prototype MCA output current indicate that output currents as high as few hundred nA can be achieved. The uniformity across the field of our first prototype, manufactured without any tolerance requirements determined by modeling was measured to be within 8%. We believe the uniformity will be within the required 2% for our next manufacturing run, as the tolerances on the structural parameters are well established at the present time.

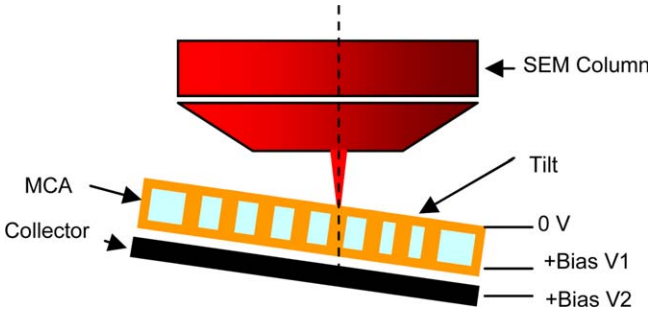

Fig. 4. Schematic diagram of experimental setup for the measurements of MCA characteristics.

Acknowledgements

This work was partially funded by DARPA Grant HR0011-05-9-0001. The authors acknowledge the very valuable technical guidance and support of Prof. F.W. Pease (Stanford University), Dr. J. Mangano (DARPA), Dr. E. Munro and Dr. J. Rouse (Munro's Electron Beam Software Ltd.), Dr. R. Stevens (Rutherford Appleton Laboratory), Dr. W.D. Meisburger (Maskless, Inc.) and Dr. D.P. Mathur (Photonics).

References

[1] D. Henry, J. Gemmink, et. al., MNE 2005, this proceedings.
[2] N.W. Parker, A.D. Brodie, et al., Proc. SPIE 3997 (2000) 713; T.H.P. Chang et al., J. Vac. Sci. B 14 (1996) 3774.
[3] B. Lin, MNE 2005, this proceedings.; H. Smith, MNE 2005, this proceedings.
[4] H. Smith, MNE 2005, Vienna, this proceedings.
[5] P.M. Shikhaliev, Nucl. Instr. Meth. A 420 (1999) 202.
[6] L. Giudicotti, Nucl. Instr. Meth. A 480 (2002) 670.
[7] G.J. Price, G.W. Fraser, Nucl. Instr. Meth. A 474 (2001) 188.
[8] A.S. Tremsin et al., Nucl. Instr. Meth. A 379 (1996) 139.
[9] C.H. Park, Nucl. Instr. Meth. A 504 (2003) 14.
[10] A.S. Tremsin, J.F. Pearson, et al., Proc. SPIE 2518 (1995) 384.